

Reinforcement Learning for Heterogeneous Teams with PALO Bounds

Roi Ceren

Department of Computer Science
University of Georgia, Athens, GA 30602
roi.ceren@gmail.com

Prashant Doshi

Department of Computer Science
University of Georgia, Athens, GA 30602
pdoshi@cs.uga.edu

Keyang He

Department of Computer Science
University of Georgia, Athens, GA 30602
kh454336@uga.edu

Abstract

We introduce reinforcement learning for heterogeneous teams in which rewards for an agent are additively factored into local costs, stimuli unique to each agent, and global rewards, those shared by all agents in the domain. Motivating domains include coordination of varied robotic platforms, which incur different costs for the same action, but share an overall goal. We present two templates for learning in this setting with factored rewards: a generalization of Perkins’ Monte Carlo exploring starts for POMDPs to canonical MPOMDPs, with a single policy mapping joint observations of all agents to joint actions (MCES-MP); and another with each agent individually mapping joint observations to their own action (MCES-FMP). We use probably approximately local optimal (PALO) bounds to analyze sample complexity, instantiating these templates to PALO learning. We promote sample efficiency by including a policy space pruning technique, and evaluate the approaches on three domains of heterogeneous agents demonstrating that MCES-FMP yields improved policies in less samples compared to MCES-MP and a previous benchmark.

1 Introduction

We focus on optimizing the performance of a team of heterogeneous agents in partially observable environments without knowledge of the environmental dynamics. An illustrative example is the robot alignment problem [12] shown in Fig. 1, where two different platforms seek to face each other by turning and emitting infrared signals, which the other detects. Here, one robot turns inexpensively due to sophisticated actuators incurring less energy cost.

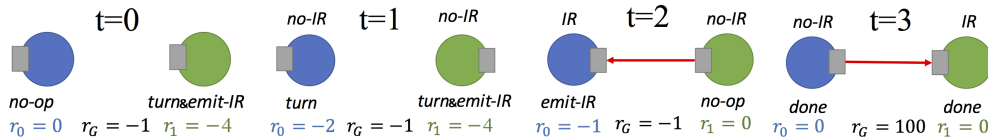


Figure 1: Illustration of a converged policy on the two-robot alignment problem yielding a trajectory where the robots align. Rewards r_0 and r_1 are local costs while r_G is the global team reward.

We consider settings comprised of two or more agents situated in a partially observable environment, where each agent receives a possibly noisy observation. Furthermore, each agent receives both a *local* reward based on the state and its individual action, as well as a *global* team reward based on all

agents’ actions. Factoring rewards into local and global components is well explored in cooperative multiagent decision making [6, 9, 13] offering the benefit that cooperation among heterogeneous agents, such as a team of varied robotic platforms, may be studied. *Both observation and rewards of each agent are communicated instantly and exactly to a centralized learner.* The joint transition, observation, and reward functions are unknown making this *model-free* RL. This form of RL is well suited for robot learning where motion noise levels are specific and usually not known.

Perkins’ [17] Monte Carlo exploring starts for partially observable Markov decision processes (POMDP) (labeled as MCEP) performs online sampling of trajectories and explores local policy neighborhoods, terminating exploration when the empirical action-values for a policy can no longer be improved by performing a different action. When leveraging sample count requirements analogous to probably approximately correct bounds, MCEP most probably arrives at an ϵ -*locally optimal* policy where ϵ is a function of the sample count and the probability [8]. MCEP offers the benefit of model-free RL with PALO guarantees in partially observable state spaces and single-agent contexts.

With MCEP as the departure point, this paper makes two main contributions. First, it introduces two templates for model-free RL in the heterogeneous setting. Our first template is a straightforward extension of MCEP, which models the problem as a canonical MPOMDP by mapping joint observation sequences to joint actions. We label it as MCEMP. The second approach, motivated by methods factoring joint-policy search spaces [1, 9], decomposes the single large policy in MCEMP to a collection of policies each mapping joint observations to individual actions. This template that performs MCEP for each agent and improves the policies only if all agents show an improvement is labeled as MCEFMP. Both these templates not only offer model-free RL in the context of MPOMDPs for the first time, they represent first methods that relate sample bounds to local optimality for RL in a popular multiagent context.

Next, we instantiate our methods with PALO bounds to provide statistical guarantees of ϵ -local optimality that relate with sample complexity. We empirically demonstrate in three cooperative problem domains that both approaches arrive at good local optima with varying domain parameters. We illustrate the comparative advantage of the decomposition in MCEFMP, providing remarkable sample complexity savings over the MCEMP instantiation. We exploit a parameterized policy search space pruning introduced previously [5], trading statistical guarantees from PALO bounds for reduction in the computational burden. In comparisons with a known method, MCEFMP is sample efficient and learns much better policies, though, as is well known, PALO guarantees limit scalability.

Our cooperative multiagent setup differs significantly from single agent settings. Furthermore, the factored rewards model structure that is well suited to robotic settings. While MCEMP is a straightforward generalization of MCEP, MCEFMP is a novel contribution. It offers much reduced sample complexity due to which it runs faster and requires less pruning.

2 Background on RL for POMDPs

Monte Carlo exploring starts for POMDPs (MCEP) [17] uses MCEP [18], a flavor of Q-learning that randomly selects state-action pairs to evaluate in the beginning. MCEP locally explores neighboring policies, those that differ by a single action, and hill climbs to those that have empirically-derived higher reward values. It explores the local neighborhood of a policy by transforming the action taken at a randomly selected observation sequence \vec{o} . After each transformation, MCEP compares the empirical reward following the transformed observation sequence, denoted by $Q_{\vec{o},a}$, against the current policy. For this, it generates a T -step sampled trajectory containing observations, actions, and rewards: $\tau = (a^0, r^0, o^1, a^1, r^1, \dots, o^{T-1}, a^{T-1}, r^{T-1})$. Let $\mathcal{R}(\tau) = \sum_{t=0}^{T-1} \gamma^t r^t$ be the discounted sum of rewards for a trajectory where $\gamma \in (0, 1)$ is the discount factor. Let $R_{pre-\vec{o}}(\tau)$ and $R_{post-\vec{o}}(\tau)$ be the cumulative rewards up to and following the observation sequence \vec{o} in a trajectory τ , respectively. The expected action-value of a policy is then:

$$Q_\pi \triangleq E^{\tau \sim \pi} [R(\tau)] = E^{\tau \sim \pi} [R_{pre-\vec{o}}(\tau) + R_{post-\vec{o}}(\tau)] = E^{\tau \sim \pi} [R_{pre-\vec{o}}(\tau)] + E^{\tau \sim \pi} [R_{post-\vec{o}}(\tau)]$$

MCEP updates the Q-value by $R_{post-\vec{o}}$ with a depreciating learning rate. At each stage, k samples are taken of the value of a current policy and of each neighboring policy. It also prevents comparing policies that have not been sampled sufficiently. If Q-values for the transformation dominate the policy by ϵ , it is accepted and the process repeats for the new policy. Termination is triggered when, after k samples of trajectories that update the Q-value of each neighbor, no neighbor dominates current policy.

An instantiation of MCES-P using Greiner’s probably approximately correct local optimization [8] allows the inclusion of PAC-like guarantees, leveraging a more refined ϵ and k . In addition, a bound on the probability of error, δ , is introduced. The sample requirement k_m and error probability bound δ change with the number of transformations m .

$$k_m \leftarrow \left\lceil 2 \left(\frac{\Lambda}{\epsilon} \right)^2 \ln \frac{2N}{\delta_m} \right\rceil \quad (1)$$

where $\delta_m \leftarrow 6\delta/9.872m^2$. Let p and q be the numbers of samples of the two policies under comparison, N is the cardinality of the set of neighboring policies. Then, error ϵ is defined as:

$$\epsilon(m, p, q) = \begin{cases} \epsilon^*(m, p) & \text{if } p = q < k_m \\ \frac{\epsilon}{2} & \text{if } p = q = k_m \\ +\infty & \text{otherwise} \end{cases} \quad \text{where } \epsilon^*(m, p) = \Lambda \sqrt{\frac{1}{2p} \ln \left(\frac{2(k_m - 1)N}{\delta_m} \right)}. \quad (2)$$

As policies differ by a single action only, N is $\mathcal{O}(|A| \frac{|\Omega|^T - 1}{|\Omega| - 1})$ — significantly less than the entire space of policies $\mathcal{O}(|A| \frac{|\Omega|^T - 1}{|\Omega| - 1})$; A and Ω are the sets of actions and observations, respectively, while T is the planning horizon.

Let π be a current policy, π' a local neighbor, $\Lambda(\pi, \pi')$ the range of their possible action-values, and R_{max}, R_{min} be the maximum and minimum possible rewards from a single step. Then,

$$\Lambda(\pi, \pi') \triangleq \max_{\tau} (Q_{\pi}(\tau) - Q_{\pi'}(\tau)) - \min_{\tau} (Q_{\pi}(\tau) - Q_{\pi'}(\tau)) \leq \sum_{t=0 \dots T-1} [(R_{max} - R_{min}) - (R_{min} - R_{max})] = \sum_{t=0 \dots T-1} 2(R_{max} - R_{min}) = 2T(R_{max} - R_{min}). \quad (3)$$

Then, let $\Lambda \triangleq \max_{\pi, \pi' \in neighbor(\pi)} \Lambda(\pi, \pi')$. The PALO instantiation of MCES-P is implemented by utilizing the redefinitions of ϵ and k_m . It terminates when no policy transformation is triggered after k_m samples, or if the current policy dominates its neighbors by $\epsilon - \epsilon^*(m, p)$ for fewer than k_m samples. Hoeffding’s inequality and Theorem 2 of Perkins [17] guarantee that the PALO instantiation converges to ϵ -locally optimal policy with probability $\geq 1 - \delta$.

3 Related Work

MCES-P has been extended to self-interested multiagent settings [5], where opponents’ policies are fixed but not known to the subject agent. It maintains beliefs over models of other agents. The self-interested setting is orthogonal to the *team* problem studied in this paper.

In the context of MPOMDPs, factored-value partially observable Monte Carlo planning [3] offers some scalability by factoring the joint *value function* to exploit structure in multiagent systems. However, this is essentially a *model-based* centralized approach that either requires prior knowledge of the environment dynamics or an augmented model involving beliefs over the transition function learned via Bayes-Adaptive MPOMDP [2]. ϵ -optimality is established for the former case but not under model uncertainty. Another related approach is Monte Carlo Q-Alternating (MCQ-Alt) [4], a quasi model-based RL method for Dec-POMDPs, where agents take turns learning given the learned policy so far of the other agent. While no model is known a priori, MCQ-Alt first estimates model parameters in the intermediate step and plans. In contrast, our methods perform model-free RL in a MPOMDP setting with simultaneously learning agents.

Finally, the infinite regional policy representation (iRPR) [14] performs model-free exploration of nonparametric policies for POMDPs. While iRPR allows an unbounded number of states, its convergence is sample-intensive requiring 10^3 samples even for the simple 1D-maze domain; this makes it a poor departure point. Additionally, parameters must be manually configured to achieve optima. However, it does outperform the model-based infinite POMDP [7].

4 Heterogeneous Teams

We focus on a system of Z heterogeneous agents cooperating toward a common goal. Specifically, $\{\mathcal{R}_1, \mathcal{R}_2, \dots, \mathcal{R}_Z\}$ is the collection of agent’s reward functions, which may differ; this defines the heterogeneity. Here, $\mathcal{R}_i : S \times A \rightarrow \mathbb{R}$, $i \in \mathcal{I}$ is an agent’s reward function, which maps state and joint action to value. An agent’s reward \mathcal{R}_i is decomposed into local costs (R_i), predicated on the joint physical state and *individual* action, and the global reward (R_G), a mapping from the joint state and joint action, as shown below.

$$\mathcal{R}_i(s, a) = R_i(s, a_i) + R_G(s, a) \quad (4)$$

Algorithm 1 MCES-MP

Require: Q-value table initialized and initial joint policy, π , that is greedy w.r.t Q-values; learning rate schedule α ; error ϵ ; and horizon T

- 1: Initialize count $c_{\vec{o}, \vec{a}} \leftarrow 0$ for all \vec{o} and \vec{a} , $m \leftarrow 0$
- 2: **repeat**
- 3: Pick joint observation history \vec{o} and joint action \vec{a}
- 4: Set π to $\pi \leftarrow (\vec{o}, \vec{a})$
- 5: Generate trajectory τ of length T online by simulating transformed joint policy $\pi \leftarrow (\vec{o}, \vec{a})$
- 6: $Q_{\pi \leftarrow (\vec{o}, \vec{a})} \leftarrow (1 - \alpha(m, c_{\vec{o}, \vec{a}})) \cdot Q_{\pi \leftarrow (\vec{o}, \vec{a})} + \alpha(m, c_{\vec{o}, \vec{a}}) \cdot \mathcal{R}_{post-\vec{o}}(\tau)$
- 7: $c_{\vec{o}, \vec{a}} \leftarrow c_{\vec{o}, \vec{a}} + 1$
- 8: **if** $\max_{\vec{a}'} Q_{\pi \leftarrow (\vec{o}, \vec{a}')} > Q_{\pi} + \epsilon(m, c_{\vec{o}, \vec{a}}, c_{\vec{o}, \pi(\vec{o})})$ **then**
- 9: $\pi(\vec{o}) \leftarrow \vec{a}'$ where $\vec{a}' \leftarrow \arg \max Q_{\pi \leftarrow (\vec{o}, \vec{a}')}$
- 10: $m \leftarrow m + 1$
- 11: Reset $c_{\vec{o}, \vec{a}} \leftarrow 0$ for all \vec{o} and \vec{a}
- 12: **until** termination

Local costs may be unique to each agent and provide a way to model the diversity between agents. For example, the global reward in Fig. 1 is 100 when the robots are aligned, otherwise -1. The local component differs between robots with the more sophisticated platform incurring a cost of 2 for turning and 1 for emitting infrared while it costs 3 for the other robot to do either.

A trajectory of T steps in this *factored reward* setting is $\tau = (\vec{a}^0, \vec{r}^0, \vec{o}^1, \vec{a}^1, \vec{r}^1, \dots, \vec{o}^{T-1}, \vec{a}^{T-1}, \vec{r}^{T-1})$. Here, \vec{a} , \vec{r} and \vec{o} are vectors of all agents' actions, rewards and observations, respectively. An agent's reward in \vec{r} , denoted by r_i , is a *tuple* of the local costs and global rewards received by i based on the components in Eq. 4, and analogously for others.

5 MCES for Factored Rewards

We introduce two model-free RL approaches for the factored-reward setting. Both generalize the MCES-P template.

5.1 Joint Policy Iteration

The class of factored reward settings with agents that cooperate may be cast into the well-known framework of multiagent POMDPs (MPOMDPs) [15]. These generalize POMDPs to multiple agents; actions and observations in a MPOMDP are a joint of the individual agent actions and observations. Importantly, the output is a *single* policy that maps joint observation sequences to joint actions.

$$\text{MPOMDP} \triangleq \langle \mathcal{I}, S, A, \Omega, T, O, \mathcal{R} \rangle$$

$\mathcal{I} = \{1, \dots, Z\}$ is the set of Z interacting agents; S is the set of physical states; $A = A_1 \times \dots \times A_Z$, is the set of joint actions where A_1, A_2, \dots, A_Z are the sets of each agent's actions. A joint action is then, $\vec{a} = \{a_1, \dots, a_Z\}$; $\Omega = \Omega_1 \times \dots \times \Omega_Z$, is the set of joint observations where $\Omega_1, \Omega_2, \dots, \Omega_Z$ are the sets of each agent's observations. A joint observation is $\vec{o} = \{o_1, \dots, o_Z\}$; $T : S \times A \times S \rightarrow [0, 1]$ is the transition function that determines how the state evolves. It maps an origin state, a joint action, and an arrival state to a probability; $O : \Omega \times S \times A \rightarrow [0, 1]$ is the observation function that gives the informativeness of the observations toward the state. It maps an observation, the arrival state, and a joint action to a probability; $\mathcal{R} : S \times A \rightarrow \mathbb{R}$. While the factored reward setting also includes the individual costs of each agent's actions, we obtain the single reward function that is needed as:

$$\mathcal{R}(s, a) = \sum_{i \in \mathcal{I}} R_i(s, a_i) + R_G(s, a) \quad (5)$$

Algorithm 1, which we call MCES for MPOMDPs (MCES-MP), straightforwardly generalizes MCES-P. It modifies MCES-P in several ways. Line 3 picks joints instead of individual observations and actions. In line 4, $\pi \leftarrow (\vec{o}, \vec{a})$ denotes the *transformed policy* that prescribes \vec{a} on encountering observation sequence \vec{o} . The trajectory τ in line 5 is as described in the previous section. Line 6 updates the Q-value by $R_{post-\vec{o}}$ with an averaging learning rate $\alpha(m, c) = \frac{1}{c+1}$, where m is the number of transformations taken so far and c the count of updates to the Q-function. In this instance, m does not affect the learning rate. To define $\mathcal{R}_{post-\vec{o}}(\tau)$ in line 6, we begin by defining $\mathcal{R}(\tau)$ as $\mathcal{R}(\tau) = \sum_{t=0}^{T-1} \gamma^t \sum_{i \in \mathcal{I}} r_i^t + r_G^t$, where r_i^t and r_G^t are the local and global components of the reward r_i at time t received by i . $\mathcal{R}_{post-\vec{o}}(\tau)$ is then the portion of $\mathcal{R}(\tau)$ that succeeds joint observation \vec{o} .

We may instantiate the MCES-MP template using PALO bounds to obtain an algorithm MCESMP+PALO that can be implemented similarly to the PALO instantiation of MCES-P. A key difference from MCES-P is that the policy maps joint observations to joint actions, due to which the size of the local policy neighborhood N^{MP} is significantly larger. Specifically,

$$N^{\text{MP}} = \prod_{i \in \mathcal{I}} |A_i| \left(\frac{\prod_{i \in \mathcal{I}} |\Omega_i|^T - 1}{\prod_{i \in \mathcal{I}} |\Omega_i| - 1} - 1 \right). \quad (6)$$

The other difference is in the maximal range of action-values of a policy π and its transformation π' , denoted as $\Lambda(\pi, \pi')$ previously. We now utilize the maximum and minimum values of the reward function defined in Eq. 5 in the computation of Λ in Eq. 3. Given these changes, the definitions of k_m and $\epsilon(m, p, q)$ as in Eqs. 1 and 2 modify to accommodate them, and the algorithm terminates similarly. MCESMP+PALO may terminate early similarly to MCES-P.

PROPOSITION 1 (PROOF FOLLOWS FROM GREINER [8]). *With probability $1 - \delta$, MCESMP+PALO iterates over a series of policies mapping joint observations to joint actions, $\pi^1, \pi^2, \dots, \pi^m$, such that the transformed policy π^{j+1} dominates the previous policy π^j in value for all agents and terminates to an ϵ -locally optimal policy π^m , where no neighbor dominates the converged policy by more than ϵ .*

5.2 Joint Transformation of Individual Policies

Motivated by previous approaches in multiagent planning that divide the joint-policy search space into individual agent policy search spaces with a coordination mechanism [1, 9], our second method seeks to learn a vector of policies, one for each agent. A policy π_i for an agent i in this vector maps joint observations of all agents to the action prescribed for i . It does not require combining the rewards as in Eq. 5; rather it continues to utilize each agent's separate reward signal r_i obtained from \mathcal{R}_i . The model-free RL is outlined in Algorithm 2, and we refer to it as MCES for factored-reward MPOMDPs (MCES-FMP).

Similar to MCES-MP, we begin by picking a joint observation history \vec{o} and action \vec{a} either randomly or in an iterated manner. However, it uses these to transform each agent's current policy by setting the action at \vec{o} with its action in \vec{a} (line 4). MCES-FMP maintains the Q-value for each agent's transformed policy (line 7) *additionally indexed by the joint of other agents' actions picked for \vec{o}* . This ensures consistent updates of Q-values for the same set of joint actions, and thus the multiagent policy vector. As such, it maintains as many Q-functions as the number of agents and combinations of other agents' actions picked for \vec{o} in the worst case, i.e., $\mathcal{O}(ZA^{Z-1})$. To obtain $\mathcal{R}_{i, \text{post}-\vec{o}}(\tau)$ in line 7 note that, $\mathcal{R}_i(\tau) = \sum_{t=0}^{T-1} \gamma^t (r_i^t + r_G^t)$. Then, $\mathcal{R}_{i, \text{post}-\vec{o}}(\tau)$ is simply the portion of $\mathcal{R}_i(\tau)$ that obtains after \vec{o} has occurred in the trajectory. Finally, the conjunction on line 10 ensures that all transformations are accepted together or none are.

Algorithm 2 MCES-FMP

Require: Q-value tables initialized and initial profile of agent policies, $\{\pi_i\}_{i=1}^Z$, that are greedy w.r.t. Q-values; learning rate schedule α ; error ϵ ; and horizon T

- 1: Initialize $c_{\vec{o}, a_i}^i \leftarrow 0$ for all \vec{o}, a_i , and $i \in \mathcal{I}, m \leftarrow 0$
 - 2: **repeat**
 - 3: Pick joint observation history \vec{o} and joint action \vec{a}
 - 4: Set π_i to neighboring policy $\pi_i \leftarrow (\vec{o}, a_i)$ for all $i \in \mathcal{I}$
 - 5: Generate trajectory τ of length T online by obtaining each agent's action using its transformed policy $\pi_i \leftarrow (\vec{o}, a_i)$ for each $i \in \mathcal{I}$
 - 6: **for all** $i \in \mathcal{I}$ **do**
 - 7: $Q_{\pi_i \leftarrow (\vec{o}, a_i)}^{\vec{a}-i} \leftarrow (1 - \alpha(m, c_{\vec{o}, a_i}^i)) \cdot Q_{\pi_i \leftarrow (\vec{o}, a_i)}^{\vec{a}-i} + \alpha(m, c_{\vec{o}, a_i}^i) \cdot \mathcal{R}_{i, \text{post}-\vec{o}}(\tau)$
 - 8: $c_{\vec{o}, a_i}^i \leftarrow c_{\vec{o}, a_i}^i + 1$
 - 9: **if** $\bigwedge_{i \in \mathcal{I}} \left(\max_{a'_i \in \mathcal{A}_i} Q_{\pi_i \leftarrow (\vec{o}, a'_i)}^{\vec{a}-i} > Q_{\pi_i}^{\vec{a}-i} + \epsilon(n, c_{\vec{o}, a_i}^i, c_{\vec{o}, \pi_i(\vec{o})}^i) \right)$ **then**
 - 10: $\pi_i(\vec{o}) \leftarrow a'_i$ where $a'_i \leftarrow \arg \max_{a'_i} Q_{\pi_i \leftarrow (\vec{o}, a'_i)}^{\vec{a}-i} \forall i \in \mathcal{I}$
 - 11: $m \leftarrow m + 1$
 - 12: Reset $c_{\vec{o}, a_i}^i \leftarrow 0$ for all \vec{o}, a_i , and $i \in \mathcal{I}$
 - 13: **until** termination
-

Consequently, MCES-MP could approach the same local optima in policies as MCES-FMP, but may follow a different path. Specifically, if any agent receives a worse individual cost, despite the

cumulative reward being better, MCES-FMP will not transform. While this may preclude higher team rewards in interim steps, the benefit is that MCES-FMP targets policies with higher joint values and takes larger steps in its search as we demonstrate in Section 7.

When instantiated with PALO bounds (MCESFMP+PALO), the policy decomposition approach provides significant sample complexity reductions. This is primarily because of a much reduced local neighborhood, where the first factor involving actions is not exponential in the number of agents (c.f. Eq. 6):

$$N^{\text{FMP}} = |A_i| \left(\frac{\prod_{i \in \mathcal{I}} |\Omega_i|^T - 1}{\prod_{i \in \mathcal{I}} |\Omega_i| - 1} - 1 \right).$$

The conjunction on line 9 of MCESFMP+PALO redefines Eqs. 1 and 2 as,

$$k_m = \left\lceil 2 \left(\frac{\Lambda(\pi_i, \pi'_i)}{\epsilon} \right)^2 \ln \left(\frac{2^Z \sqrt{4Z - 2} N^{\text{FMP}}}{2^Z \sqrt{\delta_m}} \right) \right\rceil \quad (7)$$

$$\epsilon^*(m, p) = \frac{\Lambda(\pi_i, \pi'_i)}{\sqrt{2p}} \sqrt{\ln \frac{2^Z \sqrt{(4Z - 2)(k_m - 1) N^{\text{FMP}}}}{2^Z \sqrt{\delta_m}}}. \quad (8)$$

Here, the maximum range of action values $\Lambda(\pi_i, \pi'_i)$ is computed analogously to Eq. 3 with the change that we utilize the maximum and minimum values of the reward function in Eq. 4. This range could get much narrower in comparison to the maximum range for MCESMP+PALO because the rewards for the latter are a sum of all local costs. Of course, this benefits the sample bound k_m .

PROPOSITION 2. *The sample bound for MCESFMP+PALO given in Eq. 7 is less than the sample bound for MCESMP+PALO if the following holds for all agents:*

$$\ln \left(\frac{2^Z \sqrt{4Z - 2} N^{\text{FMP}}}{2^Z \sqrt{\delta_m}} \right) < \left(1 + \frac{\sum_{i \in \bar{\mathcal{I}}} \mathcal{R}_{i, \max}}{\mathcal{R}_{i, \max} + \mathcal{R}_{G, \max}} \right)^2 \ln \frac{2N^{\text{MP}}}{\delta_m}$$

where $\bar{\mathcal{I}}$ is the set of all agents other than agent i .

Proposition 2 is derived by simplifying the condition when the sample bound for MCESFMP+PALO (Eq. 7) is smaller than that of MCESMP+PALO (Eq. 1 with $\Lambda = \Lambda(\pi, \pi')$ and $N = N^{\text{MP}}$). MCESFMP+PALO may terminate early if no neighboring policy exceeds the current value by $\epsilon - \epsilon^*(m, p)$. Its behavior is characterized by the following proposition.

PROPOSITION 3. *With probability $1 - \delta$, MCES-FMP iterates over a joint set of individual policies mapping joint observations to individual actions $\pi^1, \pi^2, \dots, \pi^m$ where every individual policy in the set $\pi^{j+1} = \langle \pi_1, \pi_2, \dots, \pi_Z \rangle$ in the neighborhood of π^j dominates each agent's previous policy in value and terminates to an ϵ -locally optimal set of policies π^m . Here no neighbor for any agent dominates the converged policy by more than ϵ without another agent receiving a worse reward.*

In proving Proposition 3, the space of errors increases multiplicatively with the number of agents. In MCES-P, the agent may make two categories of errors: *transforming* or *terminating* erroneously due to noisy samples of the local neighborhood. In MCES-FMP, one or more agents may individually make these errors, growing the number of errors by $2Z$. The neighborhoods are factored into Z individual neighborhoods. These observations and the values in Eqs. 7 and 8 result in the bound δ . Exhaustive proofs of Propositions 2 and 3 are included in the supplementary material.

In summary, MCES-MP explores policies which map joint observations to joint actions, aggregating all local costs with the global reward. MCES-FMP explores the set of independent policies mapping joint observations to individual actions, where agents receive their own local cost with the global reward. The latter yields reduced sample complexity when instantiated with PALO guarantees.

6 Joint Policy Search Space Pruning

PAC RL requires that we have k_m samples of each transformations in the local neighborhood to terminate, even those of observations that are less probable; such sequences may be due to noisy observations by one or more agents. Naturally, we may seek to avoid evaluating such transformations in order to speed up the overall search. Foregoing these portions of the local neighborhood preventing MCES from transforming to a higher value joint policy, resulting in a loss of expected value referred to as *regret*. Regret depends on two factors: the range of possible rewards on the pruned

observation sequence, and its likelihood of occurring. Even if the range of rewards is equivalent to other sequences, the regret due to avoiding the sequence reduces as it grows more improbable.

We may integrate this pruning into both Algorithms 1 and 2 as suggested by Ceren et al. [5] by taking an additional input parameter, ϕ , that is a user bound on allowable regret, and maintaining a slowly growing set \mathcal{P} of joint observation sequences that will be avoided. If a transformation is sought on an observation sequence in \mathcal{P} , then it is skipped. An observation sequence \vec{o} is added to the set if the cumulative regret due to all sequences including \vec{o} in \mathcal{P} is still less than ϕ .

We ensure that sufficient samples containing \vec{o} , $c_{\vec{o}}$, are obtained before its regret is considered by defining $\rho(c_{\vec{o}})$ as 0 if $c_{\vec{o}} \geq \frac{k_m}{2}$ and $+\infty$ otherwise. Then, ρ is simply added to ϕ .

7 Experiments

We evaluate MCESMP+PALO and MCESFMP+PALO on three domains with heterogeneous agents (see Table 1). Our first domain is the well-known team Tiger problem with 2 agents [16]. We expand this domain to include factored rewards: the global reward corresponds to the original reward function, and additionally each agent i incurs a cost of i for opening a door. The second domain is the 3-agent Firefighting previously introduced for evaluating cooperative decentralized planning [3] using 4 houses with a maximum fire intensity of 3. Agents incur two local costs: the distance between houses if they move ($\text{distance}/(10 - i)$) and the fire intensity of the target ($f_h/(10 - i)$). Our final domain is the 2- and 4-agent robot alignment problem [11] where each agent has two states and four states respectively. Robots incur local costs on turning ($-2 - i$) and emitting IR ($-1 - i$).

| Domain | Specifications (for all $\epsilon = 0.1, \delta = 0.1$) |
|----------------------------------|---|
| 2-agent Team Tiger (Tiger) | $ S = 2, A_i = 3, \Omega_i = 2, T = 5, 6, \text{Opt}=25.64, 32.11$ |
| 3-agent Firefighting (Fire) | $ S = 755, A_i = 3, \Omega_i = 2, T = 3, 4, \text{Opt}=-5.94, -4.83$ |
| 2- and 4-robot alignment (Align) | $ S = 4, A_i = 4, \Omega_i = 2, T = 4, \text{Opt}=14.39, 24.72$ |

Table 1: Parameters for the problem domains with optimal policy values. Our experiments involve domains of various sizes, and increasing numbers of agents and horizons.

In each domain, agents simultaneously act in a sequential environment with private observations that are conveyed exactly and perfectly to the centralized learner. Agents perform their actions based on the joint observation sequence as prescribed by the policy. Entire trajectory of T time steps is then sent back to the learning algorithm. Each trial is initialized with a random pairing of joint observation sequences to joint actions in MCES-MP or to individual actions in MCES-FMP.

| | | | Init. Value | Final Value | Samples | Transforms | k_m | ϕ |
|-------------|---------------|-----|--------------|-------------|--------------|------------|---------|--------|
| FMP+PAC | 2-agent Tiger | T=5 | -207.2 ± 1.2 | 20.8 ± 0.9 | 32,594 ± 227 | 37 ± 1.1 | 79,482 | 0.1 |
| | | T=6 | -279.8 ± 3.1 | 26.4 ± 0.4 | 67,914 ± 104 | 59 ± 1.2 | 144,582 | 0.1 |
| | 2-robot Align | | -210.7 ± 0.7 | 11.4 ± 0.6 | 28,139 ± 31 | 16 ± 1.4 | 56,838 | 0.1 |
| | 3-agent Fire | T=3 | -10.5 ± 0.1 | -6.4 ± 0.3 | 20,921 ± 93 | 3.4 ± 0.5 | 40,580 | 0.1 |
| | | T=4 | -12.8 ± 0.1 | -5.8 ± 0.2 | 46,235 ± 95 | 40 ± 1.8 | 108,512 | 0.1 |
| | 4-robot Align | | -246.0 ± 1.2 | 20.1 ± 0.2 | 39,256 ± 180 | 36.8 ± 0.4 | 84,651 | 0.1 |
| MP+PAC | 2-agent Tiger | T=5 | -207.2 ± 1.2 | 6.7 ± 1.1 | 33,985 ± 183 | 22 ± 1.4 | 80,484 | 0.2 |
| | | T=6 | -279.8 ± 3.1 | 8.6 ± 0.5 | 69,904 ± 177 | 36 ± 1.7 | 143,883 | 0.2 |
| | 2-robot Align | | -210.7 ± 0.7 | 2.7 ± 0.3 | 29,124 ± 32 | 10 ± 1.2 | 59,242 | 0.2 |
| | 3-agent Fire | T=3 | -10.5 ± 0.1 | -8.6 ± 1.2 | 21,940 ± 122 | 2.2 ± 0.4 | 53,904 | 0.2 |
| | | T=4 | -12.8 ± 0.1 | -9.3 ± 0.1 | 48,216 ± 155 | 26 ± 1.2 | 121,507 | 0.2 |
| | 4-robot Align | | -246.0 ± 1.2 | 6.9 ± 1.3 | 39,940 ± 101 | 33 ± 0.5 | 111,829 | 0.2 |
| BA FV-POMCP | 2-agent Tiger | T=5 | -207.2 ± 1.2 | -55 ± 1.7 | 32,993 ± 95 | - | - | - |
| | | T=6 | -279.8 ± 3.1 | 5.8 ± 0.2 | 67,884 ± 63 | - | - | - |
| | 2-robot Align | | -210.7 ± 0.7 | -20.9 ± 0.4 | 26,169 ± 18 | - | - | - |
| | 3-agent Fire | T=3 | -10.5 ± 0.1 | -8.7 ± 0.2 | 20,962 ± 80 | - | - | - |
| | | T=4 | -12.8 ± 0.1 | -9.2 ± 0.2 | 46,270 ± 84 | - | - | - |
| | 4-robot Align | | -246.0 ± 1.2 | 7.7 ± 0.1 | 40,040 ± 93 | - | - | - |

Table 2: Average metrics with std. error over 5 runs for all methods. In every case, MCESFMP+PALO significantly outperforms MCESMP+PALO and a benchmark in value of converged policy while taking similar (or fewer) samples per transform. We report the team reward of the initial and converged policies for all methods.

Comparative performances Factored-value POMCP [3] offers the previous best model-based solution of MPOMDPs. It may be combined with the Bayes adaptive approach for initial model building. We empirically validate the drastically reduced number of samples required by MCESFMP+PALO compared to MCESMP+PALO. We sought to obtain high-valued *converged* policies from the two

methods for the least regret in a reasonable amount of clock time (each run was capped at 10 hours on a typical PC). Additionally, the sample counts of the two methods are compared with those used by BA-FV-POMCP. The latter uses samples from the environment for the initial model-building phase and simulations for the model solving. As the simulations are performed using the built model, we limit our attention to the number of samples utilized for model building. We report on the values of the converged joint policies for all three methods while allowing MCESMP+PALO and BA-FV-POMCP to use a similar number of samples as MCESFMP+PALO. To permit comparison, values of policies from both methods were computed similarly: the policies were simulated and local rewards of all agents were summed and added to the global reward; this was accumulated across all steps in the trajectory. As another baseline, we implemented an algorithm that uses the single-agent MCES-P for learning the policy of each agent individually, but agents are still situated in the multiagent setting. Trajectories are generated by jointly performing the actions from each agent’s policy. Experiment data is included in the supplementary material.

Table 2 lists the metrics with the values averaged over 5 runs of each algorithm starting at differing initial policies. The ϕ that led to convergence is also reported. Observe that MCESFMP+PALO yields a joint policy that is significantly better than the joint from MCESMP+PALO and BA-FV-POMCP for about the same numbers of samples. This holds for multiple problem domains and their configurations. Furthermore, the policies generate coordination as is evident from the improvement over the MCES-P baseline. In Fig. 2 (left), we show progressions of the Q-values of the joint policies as they transform in both methods. In particular, transforms by MCESFMP+PALO are more rewarding and the difference in samples is dramatic for robot alignment.

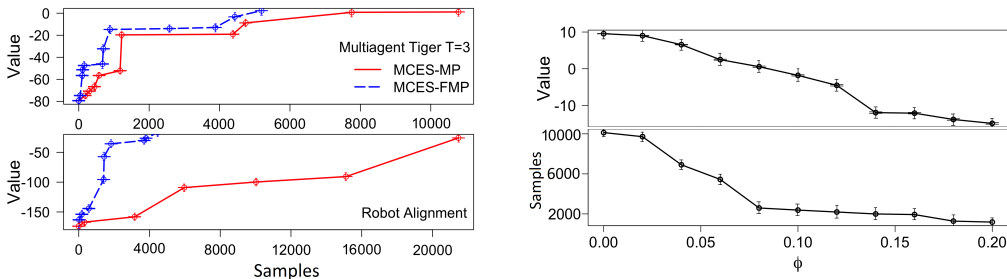


Figure 2: (left) Intermediate policy values for team Tiger $T = 3$ ($\phi = 0.05$) and 2-agent alignment ($\phi = 0.1$). MCES-FMP converges to similar or better policies than MCES-MP using far fewer samples. (right) Illustration of MCES-FMP with varying ϕ , including convergence to near-optimal values with no pruning. Each data point averages 11 runs on team Tiger $T=3$. Standard errors are very small.

Characterization of local optima MCESFMP+PALO converges to good quality policies that are close to optimal. To illustrate this, we let the allowable regret ϕ vary from 0 (no pruning) to 0.2 in the context of Tiger with $T = 3$. Figure 2 (right) shows a converged value of 10.28 for the policy vector in the absence of pruning; this gradually drops as ϕ increases. Expectedly, the number of used samples drops significantly as well. With $\phi = 0$, MCESFMP+PALO achieved policies of value -6.26 for Fire and 11.81 for Align, albeit with more samples. Figure 1 demonstrated a successful run on the particularly challenging 2-robot Align as evidence of the good-quality policies learned by MCES-FMP. The learned policy vector guides the two robots to a successful alignment.

8 Concluding Remarks

MCES-P offers elegant policy-based RL in the partially observable, single-agent context. We generalized MCES-P to a heterogeneous team setting, introducing model-free learning by searching in the space of joint policies. We presented two templates for which PAC-like guarantees were established on the local optimality of the converged policies. Empirical results on three domains with number of agents ranging from 2 to 4 comprehensively establish the positive performance of these first model-free techniques that fill an important gap in the literature on cooperative decision making.

Some interesting observations can be made about the relationship between optima in -FMP and -MP. All optima in MCES-MP are also optima in MCES-FMP, as a reduced total reward reflects a decrease in individual reward for some or all agents. However, a neighboring policy’s total reward may be higher if the cost for one agent reduces more than that incurred by another agent. In this case, -FMP will not transform while -MP will. Therefore, optima in -FMP may not be so for -MP. Even

so, in practice, -FMP may route to this policy via a different path or arrive at similarly-valued optima. While both methods search through the same joint policy space, they differ in convergence criteria.

While our method’s scalability is fundamentally limited by the growth of N^{FMP} and the sample guarantees imposed by PALO bounds, it is noteworthy that when the amount of interaction with the real environment is roughly equal, MCEs-FMP significantly outperforms the state-of-the-art method, BA FV-POMCP, while being model-free. Consequently, the relative scalability of BA FV-POMCP comes at the expense of any sample guarantees as well as actual performance. Importantly, BA FV-POMCP’s scalability may not confer pragmatic benefits, because real-world interactions often dominate learning time (consider a mobile robot collecting samples using typically slow actuators). When judged from this holistic perspective, this paper significantly advances the frontier of multiagent systems. As a next step, we are studying recent advances in using deep RL for POMDPs [10], and the challenges in generalizing the network and samples to the exponentially-harder MPOMDPs.

References

- [1] C. Amato, D. S. Bernstein, and S. Zilberstein. Optimizing memory-bounded controllers for decentralized pomdps. In *Twenty-Third Conference on Uncertainty in Artificial Intelligence (IJCAI)*, pages 1–8, 2007.
- [2] C. Amato and F. A. Oliehoek. Bayesian reinforcement learning for multiagent systems with state uncertainty. In *Workshop on Multi-Agent Sequential Decision Making in Uncertain Domains*, pages 76–83, 2013.
- [3] C. Amato and F. A. Oliehoek. Scalable planning and learning for multiagent pomdps. In *Proceedings of the Twenty-Ninth AAAI Conference on Artificial Intelligence*, pages 1995–2002, 2015.
- [4] B. Banerjee, J. Lyle, L. Kraemer, and R. Yellamraju. Sample bounded distributed reinforcement learning for decentralized pomdps. In *AAAI*, 2012.
- [5] R. Ceren, P. Doshi, and B. Banerjee. Reinforcement learning in partially observable multiagent settings: Monte carlo exploring policies with pac bounds. In *Proceedings of the 2016 International Conference on Autonomous Agents & Multiagent Systems*, pages 530–538, 2016.
- [6] Y.-h. Chang, T. Ho, and L. P. Kaelbling. All learning is local: Multi-agent learning in global reward games. In *Advances in Neural Information Processing Systems*, pages 807–814, 2004.
- [7] F. Doshi-Velez. The infinite partially observable markov decision process. In *Advances in neural information processing systems*, pages 477–485, 2009.
- [8] R. Greiner. Palo: A probabilistic hill-climbing algorithm. *Artificial Intelligence*, 84(1):177–208, 1996.
- [9] C. Guestrin, D. Koller, and R. Parr. Multiagent planning with factored mdps. In *NIPS*, volume 1, pages 1523–1530, 2001.
- [10] M. J. Hausknecht and P. Stone. Deep recurrent q-learning for partially observable mdps. *CoRR*, abs/1507.06527, 2015.
- [11] L. Kraemer and B. Banerjee. Rehearsal based multi-agent reinforcement learning of decentralized plans. In *W14-The 8th Workshop Multiagent Sequential Decision Making Under Uncertainty (MSDM 2013)*, page 24, 2013.
- [12] L. Kraemer and B. Banerjee. Multi-agent reinforcement learning as a rehearsal for decentralized planning. *Neurocomputing*, 190:82–94, 2016.
- [13] B. Liu, S. Singh, R. L. Lewis, and S. Qin. Optimal rewards in multiagent teams. In *2012 IEEE International Conference on Development and Learning and Epigenetic Robotics (ICDL)*, pages 1–8, 2012.
- [14] M. Liu, X. Liao, and L. Carin. The infinite regionalized policy representation. In *Proceedings of the 28th International Conference on Machine Learning (ICML-11)*, pages 769–776, 2011.
- [15] J. V. Messias, M. Spaan, and P. U. Lima. Efficient offline communication policies for factored multiagent POMDPs. In *Advances in Neural Information Processing Systems (NIPS)*, pages 1917–1925, 2011.

- [16] R. Nair, M. Tambe, M. Yokoo, D. Pynadath, and S. Marsella. Taming decentralized pomdps: Towards efficient policy computation for multiagent settings. In *IJCAI*, pages 705–711, 2003.
- [17] T. J. Perkins. Reinforcement learning for pomdps based on action values and stochastic optimization. In *AAAI/IAAI*, pages 199–204, 2002.
- [18] R. S. Sutton and A. G. Barto. *Introduction to reinforcement learning*. MIT Press, 1998.